Inorganic Chemistry

ARTICLE

pubs.acs.org/IC

Modeling the Mechanism of the Glutathione Peroxidase Mimic Ebselen

Sonia Antony and Craig A. Bayse*

Department of Chemistry and Biochemistry, Old Dominion University, Hampton Boulevard, Norfolk, Virginia 23529, United States

ABSTRACT: Ebselen (**1**), the quintessential mimic of the antioxidant selenoenzyme glutathione peroxidase (GPx), is a potential chemopreventative for various diseases associated with oxidative stress. Density-functional theory (DFT) and solvent-assisted proton exchange (SAPE) are used to model the complex mechanism for scavenging of reactive oxygen species by **1**. SAPE is a microsolvation method designed to approximate the role of bulk solvent in chemical processes involving proton transfer. Consistent with experimental studies, SAPE studies predict the reaction of **1** with thiol (RSH) to form a selenenyl sulfide **2** to be preferred under most conditions, with an alternate pathway through a selenoxide **3** possible at high reactive oxygen species (ROS) concentrations ([ROS] ≫ [RSH]). The reduction of **2** to the selenol **4**, known to be rate-determining in the protein, has a high SAPE activation barrier due to a strong Se···O interaction which reduces the electrophilicity of the sulfur center of the -SeS- bond of **2**. Thiols, such as dithiols and peptide-based thiols, are expected to overcome this barrier through structural features that increase the probability of attack at this sulfur. Thus, in vivo, the GPx-like pathway is the most likely mechanism for **1** under most circumstances, except, perhaps, under extreme oxidative stress where initial oxidation to **3** could compete with formation of **2**. Simple thiols, used in various in vitro studies, are predicted by SAPE modeling to proceed through oxidation of **2** to a seleninyl sulfide intermediate. Overall, SAPE modeling provides a realistic interpretation of the redox mechanism of **1** and holds promise for further exploration of complex aqueous-phase reaction mechanisms.

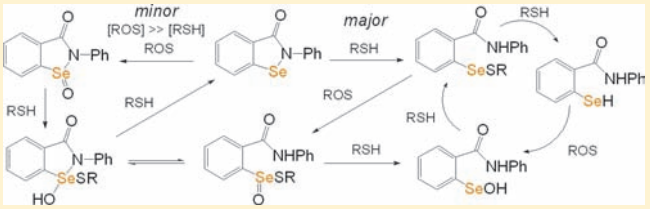

INTRODUCTION

Small organoselenium mimics of the antioxidant selenoenzyme glutathione peroxidase (GPx)[1−3] are important for their potential application to the prevention of diseases related to oxidative stress such as arthritis, cancer, and cardiovascular disease.[4−9] Specifically, ebselen **1** is a nontoxic scavenger of reactive oxygen and nitrogen species (ROS/RNS) with anti-inflammatory, antiatherosclerotic and anticytotoxic properties[10] that has been proposed as a treatment to reduce the oxidative damage produced by stroke.[11] Ebselen inhibits apoptosis[12] by reacting with peroxides in cells, membranes, lipids, and lipoproteins[13] and scavenges RNS more effectively than other common antioxidants such as ascorbate, cysteine, and methionine.[14−16] Free or protein-bound nucleophilic thiols reduce **1** to a selenenyl sulfide **2**,[10] a possible storage and transport form of the compound.[17] This reaction also inhibits enzymes that produce ROS/RNS associated with inflammation (i.e., protein kinase C, NO synthase, etc.) by blocking sulfhydryl groups.[10,16] The reaction of **1** with the cysteinate ligands of zinc−sulfur proteins releases zinc to potentially impact genomic stability.[18] Unlike naturally occurring selenium sources, **1** is not a dietary supplement for selenium[19] and is excreted as sugar derivatives.[20]

Ebselen and other organoselenium compounds catalyze the same overall reduction of ROS as GPx,[1,3] which operates by a simple, three step mechanism (Scheme 1) involving changes in the oxidation state of the active-site selenocysteine (SeCys) residue. ROS oxidize the resting state selenol (GPx-SeH) to the selenenic acid (GPx-SeOH) which is reduced to the selenol by 2 equiv of glutathione (GSH) through a selenenyl sulfide intermediate (GPx-SeSG). These intermediates have been characterized experimentally by ^{77}Se NMR spectroscopy except for GPx-SeOH which is air-oxidized to the seleninic acid (GPx-SeO_2H).[21] In contrast, the covalent Se−N bond of selenenamide **1** requires more complex catalytic pathways for redox cycling than GPx.[22] This feature and the close proximity of highly conserved nitrogen-containing amino acids to SeCys in GPx[21] and the semisynthetic protein selenosubtilisin[23] led to the development of a number of synthetic GPx mimics incorporating bonding and nonbonding Se···N,O interactions (e.g., cyclic selenenamides,[24] diaryl diselenides,[25−31] cyclic seleninates,[32−34] and selenuranes[35,36]).

Various groups have proposed mechanisms of ROS-scavenging by **1** based on experimentally observed intermediates and products (compiled in Scheme 2).[10,2,1,3] When thiols are abundant, **1** is converted to **2**, but catalysis through a GPx-like cycle is slowed by competition between reduction to selenol **4** and thiol exchange (eq 1).[37] The diselenide **7**, formed by the disproportionation of **2** as a rate-determining step,[27] has been proposed as the resting state for ROS-scavenging through oxidation of **7** to selenenic and seleninic acids **5** and **10**.[3] Earlier work by Fischer and Dereu suggests that thiol-reduction of **3** regenerates **1** through either a seleninyl sulfide (**6**) or a selenurane (**9**)

Received: July 26, 2011
Published: November 07, 2011

dx.doi.org/10.1021/ic201603v | *Inorg. Chem.* 2011, 50, 12075–12084

Scheme 1. ROS Scavenging Mechanism of GPx

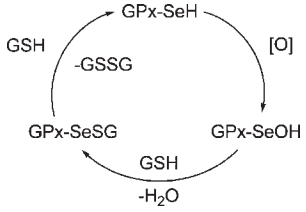

Scheme 2. Compilation of Proposed Mechanisms for the Catalytic Activity of 1

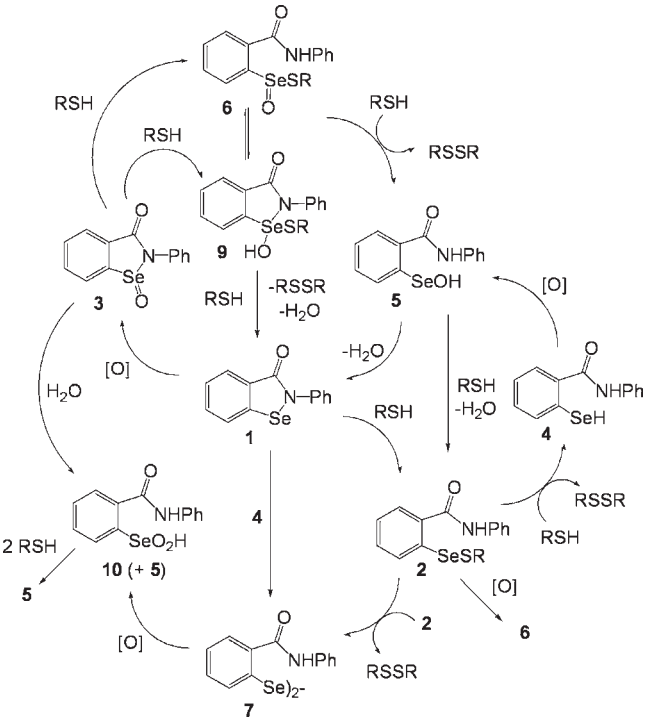

intermediate that could not be detected by NMR spectroscopy.[22] More recently, Sarma and Mugesh proposed that **1** is oxidized to an unstable selenoxide **3** which hydrolyzes to **10**.[38] Given these wide variations in proposed mechanisms and the difficulty of monitoring the many reactions and multiequilibria processes,[15] theoretical models of the mechanistic steps are invaluable for understanding the antioxidant mechanism of **1** and other organoselenium compounds.

$$RSeSR' + R''SH \rightarrow RSeSR'' + R'SH \quad (1)$$

Although various groups have used density-functional theory (DFT) to model individual steps of the ebselen mechanism,[39−43] a comprehensive analysis of the full mechanism has yet to be reported. The challenge to quantum-chemical modeling of ROS-scavenging by **1** is how to represent the proton exchange processes inherent to the individual mechanistic steps in Scheme 2 using gas-phase DFT models. In the aqueous phase, the bulk water acts as a mild acid/base catalyst to assist proton transfer between heavy atoms. This indirect, through-solvent transfer is often replaced in gas-phase models by a direct transfer from one heavy atom to another resulting in highly strained transition states and unrealistically large activation energies. These barriers are symptomatic of the direct proton exchange model and cannot be remedied by solvation corrections that seek to reproduce the electrostatic and cavity effects of solvation. To approximate the role bulk water plays in solution-phase proton-transfer processes, our group[43−46] and others (e.g., refs 47−54) have included clusters of explicit water molecules in the gas-phase model to provide an indirect pathway for proton exchange. We refer to this microsolvation technique as solvent assisted proton exchange (SAPE) to distinguish it from methods of explicit solvation designed to account only for solvation effects. Activation barriers for the GPx-like cycle of PhSeH[44] obtained from SAPE modeling are comparable to the limited available experimental data and DFT models of the truncated GPx active site of Prabhakar et al.[55] SAPE modeling of ebselen oxidation (**1**→**3**), a potentially important reaction in the scavenging of ROS/RNS, also correlates to the experimental rate constant and previous studies of oxygen atom transfer to organoselenium compounds.[43] These DFT-SAPE models are used in the following study to explore the mechanism of ROS scavenging by ebselen (Scheme 2).

THEORETICAL METHODS

DFT geometry optimizations and frequency calculations were performed using Gaussian 03[56] and the mPW1PW91[57] exchange correlation (xc) functional. Models of the reduction of MeSeOH by MeSH using a two-water SAPE network show that SAPE-derived DFT activation parameters are sensitive to the admixture of Hartree−Fock (HF) exchange.[58] The mPW1PW91 xc functional provided the best agreement of several tested functionals with the post-HF methods.[58] Generally, DFT methods with 20−25% HF exchange provide activation barriers similar to post-HF ab initio methods (MP2 and CCSD). Pure functionals underestimate and hybrid functionals with greater percentages of HF exchange overestimate the activation barriers for selenol/selenolate oxidation,[59] MeSeOH reduction,[58] and the epoxidation of alkenes by H_2O_2.[48] For the SAPE models of the reactions in Scheme 2, the selenium center was represented by the Ermler−Christiansen relativistic effective core potential (RECP) basis set[60] with added s-, p-, and d-type diffuse functions. The Wadt−Hay RECP basis set[61] augmented with diffuse functions was used for sulfur. Hydrogen centers involved in the SAPE network or bonded to a heteroatom were assigned Dunning's split-valence triple-ζ basis set with polarization functions (TZVP).[62] Hydrocarbon fragments were assigned double-ζ basis sets with polarization functions included for carbon.[63] All transition states have one imaginary vibrational mode consistent with motion along the appropriate reaction coordinate. Reported energies include zero-point energy, thermal, entropy, and solvation corrections. Note that entropy corrections are based on the harmonic oscillator approximation and may be unreliable. Solvation effects were calculated using the polarizable continuum model (PCM)[64] for water (ε = 78.39). The atomic polar tensor (APT) method was used to calculate atomic charges from the derivatives of molecular dipole moment with respect to atomic position.[65]

RESULTS AND DISCUSSION

SAPE modeling of ROS-scavenging by **1** (Scheme 2) using MeOOH and MeSH (R = Me in Scheme 2) as the model oxidant and reductant is discussed in three sections: (a) initial oxidation/reduction of **1**, (b) the GPx-like cycle, and (c) reactivity under high oxidant concentration. The homodiselenide **7** has been proposed as an important intermediate[3,22,66,67] based upon rapid diselenide formation from either **1** and **4**[68] or **2** and **4**[66] under

dx.doi.org/10.1021/ic201603v |Inorg. Chem. 2011, 50, 12075–12084

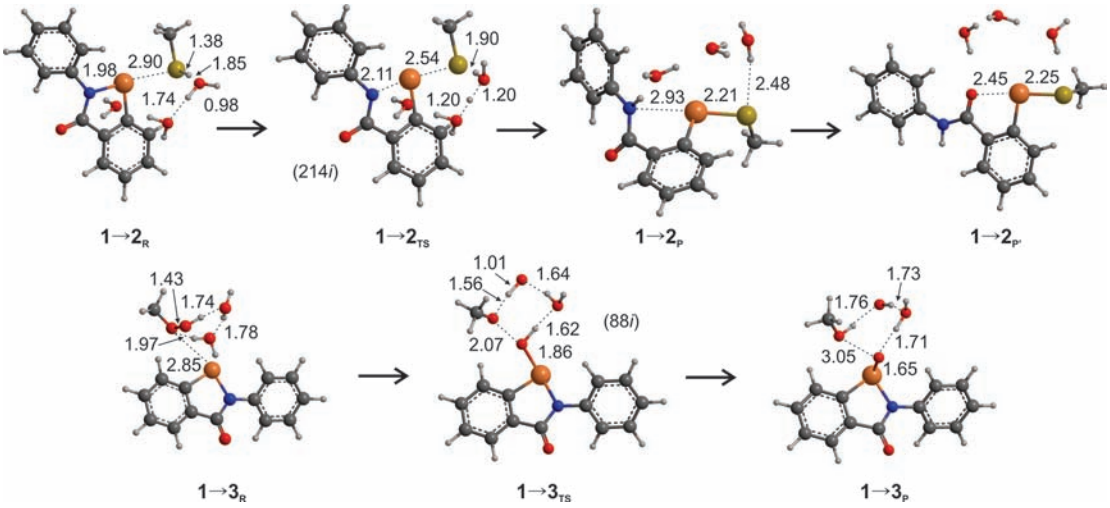

Figure 1. Selected bond distances (Å) for steps **1**→**2** (A) and **1**→**3**[43] (B). Imaginary vibrational modes for transition states are given in parentheses (cm^{-1}).

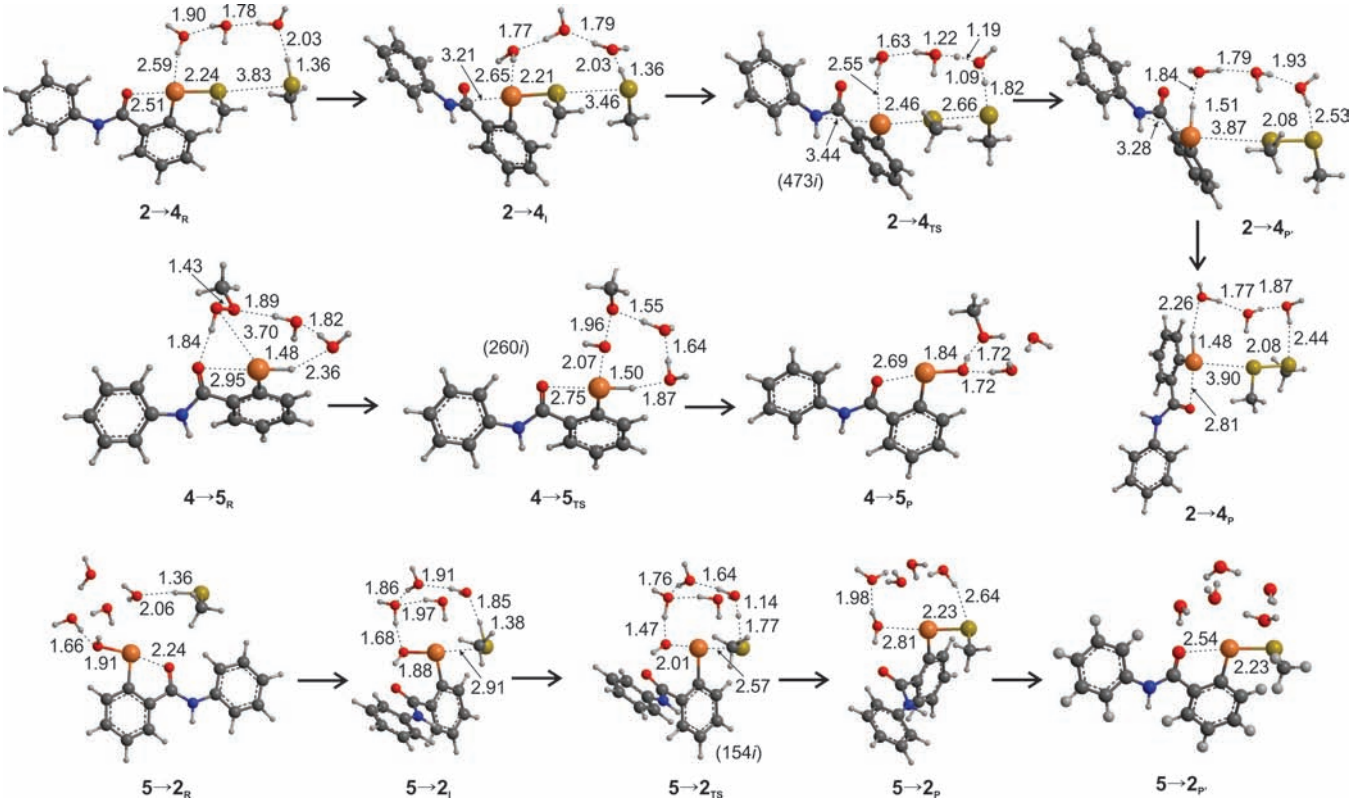

Figure 2. Selected bond distances (Å) for the GPx-like cycle for ebselen derivatives (**2**→**4** (A), **4**→**5** (B), and **5**→**2** (C)). Imaginary vibrational modes for transition states are given in parentheses (cm^{-1}).

stoichometric or substoichiometric proportions of reactants, or the slow[17,22] disproportion of 2 equiv of **2**.[3] However, diselenides are unlikely to occur in vivo due to the high concentration of nucleophiles,[69,70] and the selenol **4**, not **7**, is observed under conditions of excess GSH or dithiol.[67,71] Further, selenenyl sulfide **2** (R = Ph) can be isolated in pure form,[27] implying that its rate of disproportionation to **7** is not sufficient to sustain catalysis. Further, the rate of diselenide bond formation is second order in the concentration of organoselenium intermediates and, therefore, will be significantly slower than steps that are first order in [Se]. Because catalysis is unlikely through an intermediate formed through the biomolecular reaction of 2 equiv of catalyst, pathways that include **7** have been excluded from our study.

The SAPE microsolvation models for the mechanistic pathways in Scheme 2 were created to facilitate indirect proton exchange through a hydrogen-bonded network of 2−4 water molecules.

dx.doi.org/10.1021/ic201603v |*Inorg. Chem.* 2011, 50, 12075–12084

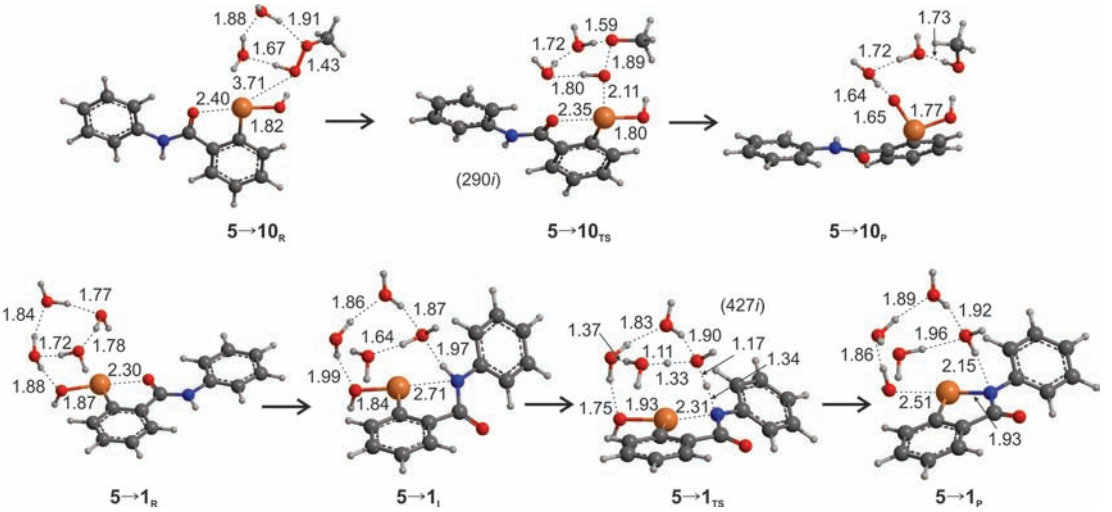

Figure 3. Selected bond distances (Å) for steps **5**→**10** (A) and **5**→**1** (B). Imaginary vibrational modes for transition states are given in parentheses (cm^{-1}).

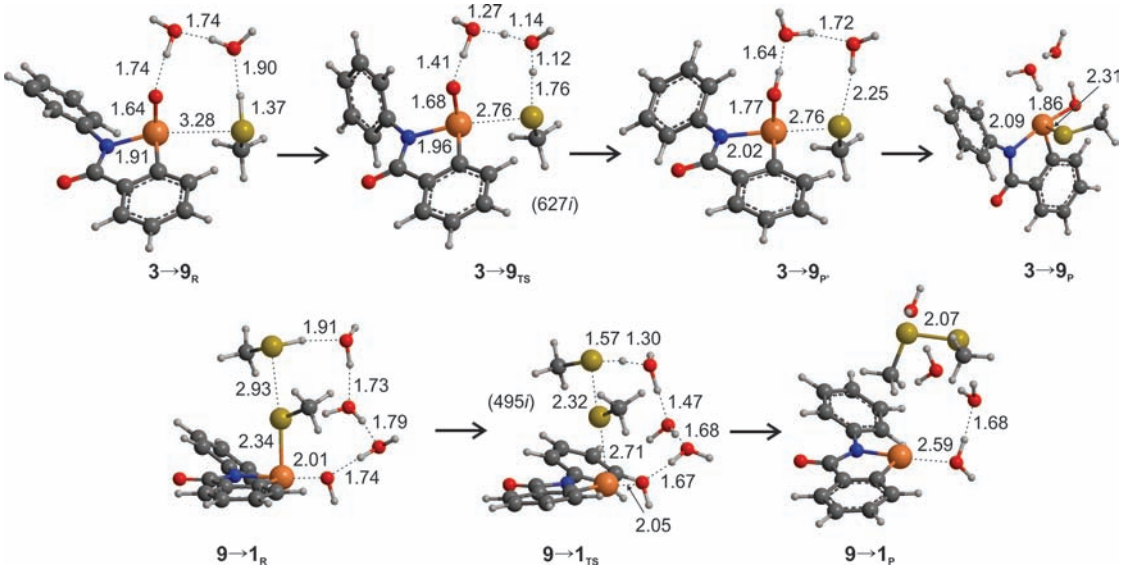

Figure 4. Selected bond distances (Å) for steps **3**→**9** (A) and **9**→**1** (B). Imaginary vibrational modes for transition states are given in parentheses (cm^{-1}).

The limited size of the SAPE network allows for manual conformation searches at the expense of a concerted pathway. Although proton-exchange reactions are considered to be stepwise processes in solution, in SAPE models proton transfer is necessarily concerted with heavy atom bond breaking/forming because the limited number of solvent molecules cannot adequately delocalize the proton charge to allow for a charge-separated intermediate. The SAPE-derived concerted transition state is expected to be an upper bound to the activation barrier of the rate-determining step of the stepwise mechanism. In the following discussion, stationary-state reactant, intermediate, transition state, and product complexes are indicated by R, I, TS, and P respectively (Figure 1−6). For example, **1**→$\mathbf{2}_{\mathbf{R}}$ represents the reactant complex in the reaction step **1**→**2**. Relative energies of these species are reported in the text as the solvation-corrected (PCM) Gibbs free energy ($\Delta G + \Delta G_{solv}$) relative to the reactant complex of the mechanistic step. These values and the uncorrected energetics (ΔH and ΔG) are listed in Tables 1−2.

Initial Oxidation/Reduction of Ebselen. In vivo, **1** undergoes reduction to selenenyl sulfide **2** or oxidation to selenoxide **3** depending upon the relative concentrations of thiol and ROS. The reaction with thiol is the preferred pathway under most conditions because **1** reacts rapidly with GSH and other thiols to form **2**[66,72] even at −70 °C[22] and, when administered intravenously, more than 90% of **1** is bound to the cysteine thiols of serum albumin.[69] Under conditions of oxidative stress, **1** may be preferentially oxidized to the selenoxide **3** as observed by Fischer and Dereu for the reaction of **1** with H_2O_2.[22] However, the major product of the treatment of **1** with a 1:1 mixture of thiol and peroxynitrite is **2** with only a small amount of **3** observed.[15] Recent studies by Sarma and Mugesh suggest that **3** is unstable and undergoes hydrolysis to seleninic acid **10**.[38]

dx.doi.org/10.1021/ic201603v |*Inorg. Chem.* 2011, 50, 12075–12084

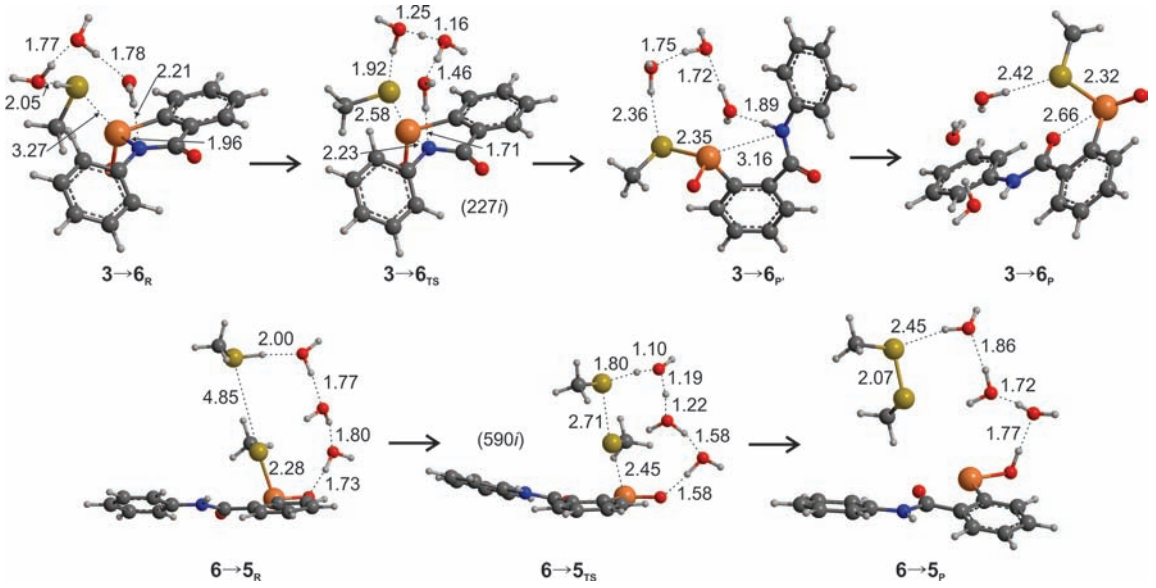

Figure 5. Selected bond distances (Å) for steps **3**→**6** (A) and **6**→**5** (B). Imaginary vibrational modes for transition states are given in parentheses (cm^{-1}).

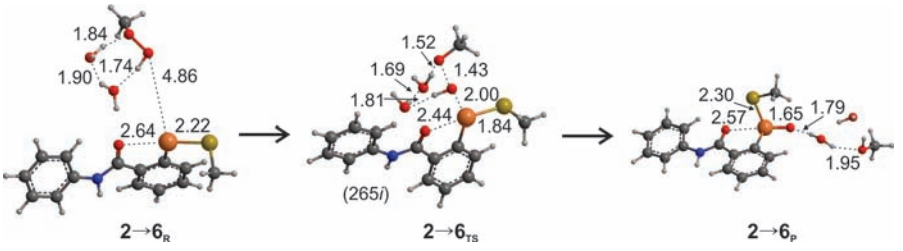

Figure 6. Selected bond distances (Å) for step **2**→**6**. Imaginary vibrational modes for the transition state is given in parentheses (cm^{-1}).

The pathway **1**→**2** was modeled from a reactant complex **1**→$\mathbf{2_R}$ (Figure 1) in which a three-water SAPE network connects the MeSH proton to the selenenamide nitrogen of **1**. The TS **1**→$\mathbf{2_{TS}}$ was determined by mapping the S−H bond-breaking coordinate to the point at which a proton relayed through the SAPE network from the thiol to the selenenamide nitrogen and the Se−S distance and Se−N distance have decreased and increased by 0.36 Å and 0.17 Å, respectively. The low activation barrier for this process (8.4 kcal/mol) relative to step **1**→**3** (17.8 kcal/mol)[43] is consistent with the product distribution of **1** in the presence of thiols and peroxides and the requirement of substantial excess oxidant for formation of **3**. Following the reaction coordinate to the product produces the selenenyl sulfide **2** with a weak intramolecular Se···N donor−acceptor interaction (2.93 Å) between the amide and the Se−S bond (Figure 1). Intramolecular interactions are important to selenium chemistry and have been examined for their potential role in tuning GPx-like activity.[2] Our study of the relative strengths of Se···N,O interactions with amides showed that the Se···O donor−acceptor interaction with the carbonyl oxygen is stronger than the Se···N interaction because of the weak Lewis basicity of the amide nitrogen group.[73] Geometry optimizations of the two isolated conformers of **2** showed that the one with an Se···O interaction ($\mathbf{2_O}$) is 3.6 kcal/mol lower than that with an Se···N interaction ($\mathbf{2_N}$), has a stronger interaction as reflected in the Natural Bond Order (NBO)[74] donor−acceptor energies ($\Delta E_{d\rightarrow a}$ = 14.0 ($\mathbf{2_O}$); 2.1 ($\mathbf{2_N}$) kcal/mol), and a shorter Se···N,O distance (2.52 ($\mathbf{2_O}$) versus 3.01 Å ($\mathbf{2_N}$)). An alternate geometry of the product complex (**1**→$\mathbf{2_{P'}}$, −21.3 kcal/mol) incorporating $\mathbf{2_O}$ is 6.9 kcal/mol more stable than **1**→$\mathbf{2_P}$.

GPx-Like Cycle. For ROS scavenging through a GPx-like cycle analogous to Scheme 1, **1** acts as a procatalyst activated by thiol reduction to **2** (Scheme 2) which is further reduced to **4** by a second equivalent of thiol. Oxidation of the selenol **4** to **5** is followed by thiol reduction to regenerate **2**. Experimental data and theoretical calculations suggest that the reduction of the selenenyl sulfide (**2**→**4**) is the rate determining step.[55] Bhabak and Mugesh have proposed that thiol exchange (eq 1) competes with this step to explain the relatively low GPx-like activity of **1**.[37] The Se···O intramolecular interaction in $\mathbf{2_O}$ ($\Delta E_{d\rightarrow a}$ = 14.0, 19.0 (DFT(B3LYP)/6-31G*)[37] kcal/mol; *d*(Se−O) = 2.52, 2.47 (DFT(B3LYP)/6-31G*)[37] Å), enhanced by aromatic stabilization,[75,76] increases the partial negative charge at the sulfur center to favor nucleophilic attack at Se.[37] In contrast, **2**→**4** is not the rate determining step[66] with dithiols such as dihydrolipoic acid because steric factors favor attack at sulfur. Additionally, Bhabak and Mugesh have shown that tert-amide based diselenides are 10−20 times more effective than sec-amide-based diselenides (i.e., **7**) because steric interactions between the amide $-NR_2$ group and the phenyl ring prevent the strong intramolecular Se···O interactions.[27] Our SAPE study of the GPx-like cycle of aryl selenols showed that weak

dx.doi.org/10.1021/ic201603v |*Inorg. Chem.* 2011, 50, 12075–12084

Table 1. Energetics of Initial Reduction (1→2) and Oxidation (1→3) of Ebselen, the GPx-Like Cycle (2→4, 4→5, 5→2), and Side Reactions of the Selenenic Acid Intermediate (5→10, 5→1)

1→2		TS	P	P′
ΔH		7.2	−13.0	−12.1
ΔG		13.6	−13.0	−13.1
$\Delta G + \Delta G_{solv}$		8.4	−14.4	−21.3
1→3[43]		TS	P	
ΔH		16.6	−37.5	
ΔG		19.1	−37.1	
$\Delta G + \Delta G_{solv}$		16.9	−41.0	
2→4	I	TS	P′	P
ΔH	3.4	18.1	8.7	6.0
ΔG	3.8	26.4	10.6	7.6
$\Delta G + \Delta G_{solv}$	8.8	31.7	14.1	11.8
4→5		TS	P	
ΔH		18.8	−65.5	
ΔG		22.7	−63.9	
$\Delta G + \Delta G_{solv}$		12.8	−68.0	
5→2	I	TS	P	
ΔH	4.1	6.9	−17.7	−22.6
ΔG	6.4	12.1	−15.4	−23.1
$\Delta G + \Delta G_{solv}$	7.5	13.1	−14.6	−18.7
5→10		TS	P	
ΔH		18.5	−34.1	
ΔG		21.1	−36.2	
$\Delta G + \Delta G_{solv}$		18.5	−37.4	
5→1	I	TS	P	
ΔH	5.4	16.1	−1.9	
ΔG	8.3	23.3	0.0	
$\Delta G + \Delta G_{solv}$	14.4	28.5	5.7	

Se···N,O interactions could be easily displaced to allow **2→4** to proceed.[76]

The SAPE models for reaction **2→4** and other steps in the GPx cycle (Figure 2 and Table 1) were based upon analogous models of steps in the GPx-like cycle of benzeneselenol.[44] In the reactant complex **2→4$_R$**, a three-water network was used to facilitate proton exchange from the thiol to the selenium center of **2**.[44] The S···S interaction (d(S−S) = 3.83 Å) between MeSH and **2** in **2→4$_R$** is weak because of the high sulfur charge induced by the strong Se···O interaction. Displacement of the amide carbonyl from the selenium in intermediate complex **2→4$_I$** requires 8.8 kcal/mol and reduces q_S for **2** by 0.30e (APT) to allow for a stronger S···S interaction (d(S−S) = 3.46 Å). The structure of **2→4$_{TS}$** and its barrier calculated from **2→4$_I$** (22.9 kcal/mol) are comparable to the analogous step for PhSeH (21.7 kcal/mol).[44] Calculated from **2→4$_R$**, the high activation barrier (31.7 kcal/mol) is consistent with the slow rate of conversion by sec-amide GPx mimics attributed to thiol exchange (eq 1) by Mugesh et al.[27,37] The product complex (**2→4$_{P'}$**) mapped from the TS has the carbonyl oxygen hydrogen bonded to the SAPE network. Rotating about the C−Se bond axis to form an Se···O interaction with the selenol of **4** (**2→4$_P$**) stabilizes the structure (−2.3 kcal/mol relative to **2→4$_{P'}$**) for an overall

Table 2. Energetics for Mechanistic Steps Following Initial Oxidation (3→9, 9→1, 3→6, 6→5) and the Oxidation of the Selenenyl Sulfide (2→6)

3→9	TS	P′	P
ΔH	5.6	−2.3	−5.8
ΔG	10.3	1.3	−1.3
$\Delta G + \Delta G_{solv}$	7.3	0.6	0.1
9→1	TS	P	
ΔH	1.4	−32.3	
ΔG	6.3	−35.3	
$\Delta G + \Delta G_{solv}$	6.5	−34.0	
3→6	TS	P′	P
ΔH	13.9	−19.1	−20.1
ΔG	19.5	−16.4	−17.9
$\Delta G + \Delta G_{solv}$	9.2	−16.0	−18.8
6→5	TS	P	
ΔH	10.9	−18.9	
ΔG	18.2	−17.3	
$\Delta G + \Delta G_{solv}$	18.4	−15.4	
2→6	TS	P	
ΔH	23.9	−31.7	
ΔG	28.7	−31.4	
$\Delta G + \Delta G_{solv}$	21.3	−34.6	

endergonic reaction (ΔG = 11.8 kcal/mol). The contrast between GSH, dithiols, and simple thiols for this step should be noted. GSH and dithiols rapidly reduce **2** whereas simple thiols such as PhSH and benzyl mercaptan do not. Dithiols convert **2→4** to a unimolecular process in which the competing pathway for thiol exchange is sterically and kinetically disfavored. Sarma and Mugesh showed that **2$_{SN}$** synthesized from an ortho-substituted aromatic thiol with S···N interactions favors selenol production of selenol **4** via thiol attack at the sulfur center.[37] Similarly, S···O interactions with carbonyls on the GSH backbone may enhance nucleophilic attack at the sulfur center to lower the barrier for **2→4**. For example, the calculated APT charges of **2$_{SN}$** (−0.16e) and **2$_{pep}$** (−0.21e) are less negative than the model selenenyl sulfide in our SAPE studies (R = Me, −0.24e) suggesting that GSH and related thiols favor the **2→4** path, but would be less effective than Mugesh's synthetic thiol because of the weaker S···O interaction. The lack of similar interactions in simple thiols prevents effective ROS scavenging through a GPx-like cycle and alternate pathways for reaction must be considered.

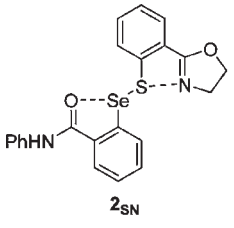

2$_{SN}$

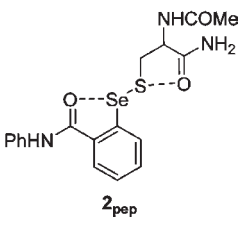

2$_{pep}$

Under the GPx-like mechanism, available oxidants convert selenol **4** to the selenenic acid **5**. In the reactant complex **4→5$_R$**, hydrogen bonding of the MeOOH proton to the amide carbonyl anchors the oxidant close to the selenium center (d (Se−O) = 3.70 Å). From this complex, the transition state

dx.doi.org/10.1021/ic201603v |*Inorg. Chem.* 2011, 50, 12075–12084

($\mathbf{4}\rightarrow\mathbf{5}_{TS}$) is found at Se−O and O−O distances of 2.07 and 1.96 Å, respectively, with an imaginary frequency (260i cm^{-1}) corresponding to the appropriate bond breaking/forming coordinates. The calculated barrier (12.8 kcal/mol) is lower than that for the PhSeOH (19.1 kcal/mol)[44] because of the increased solvation of the TS in the ebselen intermediate ($\Delta G^{\ddagger}_{sol}$ = 9.9 kcal/mol) similar to that calculated for other ortho-substituted selenols.[76] The lower barrier for $\mathbf{4}\rightarrow\mathbf{5}_{TS}$ in comparison to oxidation of **1**[43] agrees with the relative experimental rate constants for the H_2O_2-oxidation of these species (**1** (0.29 $mM^{-1}min^{-1}$ and **4** (2.8 $mM^{-1}min^{-1}$)).[77] The overall reaction is exothermic (−65.4 kcal/mol) forming the product complex $\mathbf{4}\rightarrow\mathbf{5}_{P}$ with selenenic acid stabilized by a Se···O interaction (2.35 Å).

Selenenic acids are rapidly reduced to selenenyl sulfides ($\mathbf{5}\rightarrow\mathbf{2}$) or oxidized to seleninic acids ($\mathbf{5}\rightarrow\mathbf{10}$) as shown by Goto et al for a sterically hindered stable selenenic acid.[78] Thiol reduction of ebselen selenenic acid ($\mathbf{5}\rightarrow\mathbf{2}$) completes the GPx-like cycle and was modeled as an S_N2-type backside attack of the thiol on Se to eliminate H_2O. Reduction of internally stabilized selenenic acids such as **5** with its Se···O interaction trans to the −OH leaving group must first displace the donor group for the reaction to proceed via a backside attack.[76] Intermediate complex $\mathbf{5}\rightarrow\mathbf{2}_{I}$ (Figure 2), in which the Se···O interaction of $\mathbf{5}\rightarrow\mathbf{2}_{R}$ is replaced by an Se···S interaction with MeSH and the amide carbonyl rearranged to hydrogen bond to the SeOH proton, is 7.5 kcal/mol higher than $\mathbf{5}\rightarrow\mathbf{2}_{R}$. From $\mathbf{5}\rightarrow\mathbf{2}_{I}$, the S−H bond-breaking coordinate was followed to relay the thiol proton through the SAPE network to the leaving −OH group and form $\mathbf{5}\rightarrow\mathbf{2}_{P}$ (−14.6 kcal/mol). Formation of an Se···O interaction to **5** in $\mathbf{5}\rightarrow\mathbf{2}_{P'}$ stabilizes the product by an additional 4.1 kcal/mol. The barrier calculated from $\mathbf{5}\rightarrow\mathbf{2}_{I}$ (5.6 kcal/mol) is comparable to the value calculated for the conversion of PhSeOH to PhSeSMe (6.6 kcal/mol)[44] with an overall higher barrier from the reaction complex (13.1 kcal/mol) because of stabilization of the selenenic acid group by the Se···O interaction. This moderate barrier is consistent with the rapid reaction of **5** in the presence of thiols.[38] The overoxidation of **5** ($\mathbf{5}\rightarrow\mathbf{10}$, Figure 3 and Table 1) was modeled as an oxygen-atom transfer from MeOOH facilitated by a two-water network. From $\mathbf{5}\rightarrow\mathbf{10}_{R}$, the attacking oxygen approaches selenium perpendicular to the Se−OH plane with the resulting activation barrier for $\mathbf{5}\rightarrow\mathbf{10}_{TS}$ (18.5 kcal/mol) and reaction energy to $\mathbf{5}\rightarrow\mathbf{10}_{P}$ (−37.4 kcal/mol) comparable to the SAPE-derived energetics of the oxidation of **1** and other organoselenium species.[43] Comparing the energetics of the competing reactions that selenenic acid may undergo, the oxidation of **5** would be favored under conditions of oxidative stress ([ROS] ≫ [thiol]), otherwise $\mathbf{5}\rightarrow\mathbf{2}$ with its lower barrier (13.1 kcal/mol) is preferred.

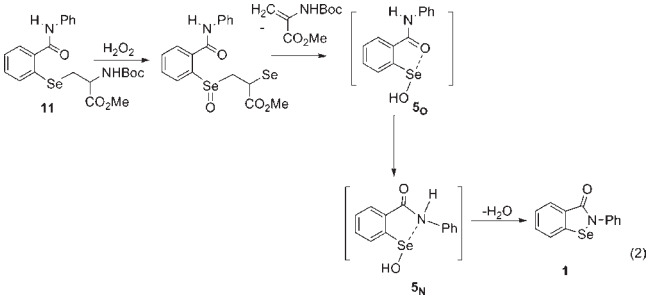

Fisher and Dereu have suggested that condensation of selenenic acids to selenenamides (i.e., $\mathbf{5}\rightarrow\mathbf{1}$) is favorable for **1** and GPx in the absence of reducing thiols.[22] Cyclic selenenamides and seleninic acids are the major products of the H_2O_2-oxidation of **7** and related sec-amide-based diselenides because of the availability of an adjacent −NHR group.[3] Ebselen seleninic acid **10** may also be converted to **1** through partial reduction to **5**.[38] Similarly, Mugesh et al. have shown that **1** is a product of selenoxide elimination from the *Se*-arylselenocysteine **11** (eq 2).[38] Dehydration of the selenenic acid ($\mathbf{5}\rightarrow\mathbf{1}$) is expected to occur through intermediate $\mathbf{5}_{N}$ in which the amide nitrogen forms a donor−acceptor interaction with the Se−OH bond. This conformer is less stable than $\mathbf{5}_{O}$ (ΔG = 8.4 kcal/mol) where the carbonyl oxygen forms a stronger Se···O interaction (NBO: $\Delta E_{d\rightarrow a}$ = 23.2 kcal/mol versus 3.5 kcal/mol). An intermediate reactant complex $\mathbf{5}\rightarrow\mathbf{1}_{I}$ was constructed by adding a square four-water SAPE network to $\mathbf{5}_{N}$ to provide a path for proton transfer from the amide proton to the selenenic acid hydroxyl group (Figure 3). Rearrangement of this intermediate to the reactant complex based upon $\mathbf{5}_{O}$ ($\mathbf{5}\rightarrow\mathbf{1}_{R}$) requires more energy than the displacement of the Se···O interaction in step $\mathbf{2}\rightarrow\mathbf{4}$ (14.4 kcal/mol versus 8.8 kcal/mol) because of the stronger Lewis basicity of the selenenic acid. The TS $\mathbf{5}\rightarrow\mathbf{1}_{TS}$, located by mapping the N−H bond-breaking coordinate from $\mathbf{5}\rightarrow\mathbf{1}_{I}$, leads to Se−N bond formation and loss of water ($\mathbf{5}\rightarrow\mathbf{1}_{P}$, ΔG = 5.7 kcal/mol). This proton transfer from the more basic amide to the hydroxyl group is a high barrier process (28.5 kcal/mol relative to $\mathbf{5}\rightarrow\mathbf{1}_{R}$) relative to selenenic acid reduction ($\mathbf{5}\rightarrow\mathbf{2}$) consistent with cyclization under thiol-free conditions.[22] Note that the transition state for the SAPE model is substantially lower than that determined by direct proton transfer.[38]

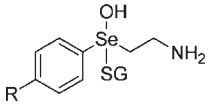

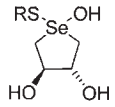

Pathways under Highly Oxidizing Conditions. The activity of **1** as a ROS scavenger in spite of the high barrier obtained for step $\mathbf{2}\rightarrow\mathbf{4}$ of the GPx-like cycle may suggest that the molecule's antioxidant properties may be more effective under conditions of oxidative stress (e.g., $rate_{1\rightarrow3} > rate_{1\rightarrow2}$). Fischer and Dereu showed that **1** is regenerated from **3** by 2 equiv of thiol.[22] Mechanistic pathways were proposed through either seleninyl sulfide **6** or the hypervalent selenurane **9**, but neither of these intermediates could be detected experimentally.[22] Related thioselenurane intermediates **12** and **13** have been proposed as intermediates in the ROS scavenging of selenides.[79,80] **12** was confirmed by Cowan et al. by mass spectrometry, but could not be detected by NMR.[79] The DFT(mPW1PW91) ^{77}Se NMR chemical shifts, determined using the gauge invariant atomic orbital (GIAO) method[81] in the gas-phase with the Se RECP basis set replaced by an all-electron representation (TZVP; i.e., BSIIa),[82,83] of intermediates **6** (1123 ppm) and **9** (839 ppm) are well-separated such that these species may be detectable if their lifetimes are greater than the NMR time scale. Thiols can easily attack the Se(IV) center of **3** to either reduce the selenoxide to **6** or form **9** without ring-opening. Pathways through **9** may be preferred because of the stability of the five-membered ring.[10] The intermediates react with a second equivalent of thiol to form the selenenic acid **5** or regenerate **1** directly. Our previous SAPE study explored the reduction of methyl- and benzeneseleninic acid[45] to the selenenic acid **17** by two possible pathways: through seleninyl sulfide **15** or by thiol addition to thioselenurane **16** (Scheme 3).

dx.doi.org/10.1021/ic201603v |*Inorg. Chem.* 2011, 50, 12075–12084

Scheme 3. Mechanism Used for DFT-SAPE Modeling of the Thiol Reduction of Seleninic Acids

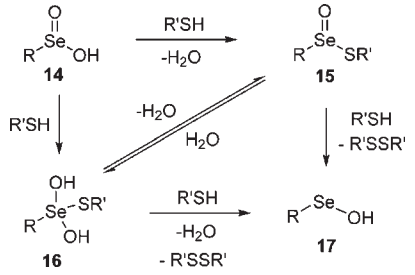

This study suggested that the first step of the reduction produces **16** which interconverts to **15** prior to subsequent reduction to **17**. The models for these steps have been adapted for the thiol-reduction of ebselen selenoxide **3** through intermediates **6** or **9**.

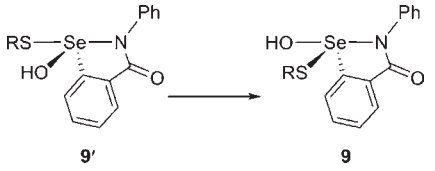

Thioselenurane formation (**3**→**9**) was modeled using a two-water SAPE network added to the donor−acceptor complex of **3** and MeSH to direct the thiol proton to the oxo group (Figure 4 and Table 2). This process for the expansion of the selenium coordination sphere through Se−S bond formation (Δd_{Se-S} = −0.52 Å) with conversion of the Se═O bond to Se−OH ((Δd_{Se-O} = +0.33 Å) is comparable to the related reaction of the seleninic acid (**14**→**16**) ($\Delta G^{\ddagger} + \Delta G_{solv}$ = 7.3 versus 7.8[45] kcal/mol). The thioselenurane in product complex **3**→$\mathbf{9_{P'}}$ formed by following the reaction coordinate is in an unstable conformation **9′** with the -SMe group trans to the amide. Pseudorotation to **9**, the conformation with a trans arrangement of the most electronegative groups (amide and hydroxyl) of the three-center-four-electron bond,[84] should be rapid.[85] The rearranged product complex **3**→$\mathbf{9_P}$ was 3.6 kcal/mol more stable than **3**→$\mathbf{9_{P'}}$ and is predicted to be in equilibrium with the reactants (0.1 kcal/mol). Further reaction of **9** with thiol would regenerate **1** through the elimination of disulfide and water. A three-water network in **9**→$\mathbf{1_R}$ bridges the thiol proton to the leaving −OH group such that the attacking thiol forms an S···S interaction collinear with the Se−S bond (d (S···S) = 2.93 Å (Figure 4)). Nucleophilic attack at the sulfur is expected to be favorable because of the distribution of groups around the positive Se(IV) center (q_{Se}(APT) = 1.52e). The inductive effect enhances the electrophilicity of the sulfur center relative to the selenenyl sulfide **2** (q_S(APT) = −0.169e (**9**) vs −0.243e (**2**)) and is reflected in the stronger S···S interaction in reactant complex **9**→$\mathbf{1_R}$ relative to **2**→$\mathbf{4_R}$ (d (S···S) = 2.93 vs 3.83 Å). The more favorable interaction also results in an early transition state **9**→$\mathbf{1_{TS}}$ (6.5 kcal/mol) at Se−S and S−S bond lengths of 2.71 Å and 2.32 Å, respectively (compare **2**→$\mathbf{4_{TS}}$: d(Se−S) = 2.46 Å and d(S−S) = 2.66 Å), consistent with the exothermicity of **9**→$\mathbf{1_P}$ (−34.0 kcal/mol).

Thiol reduction of **3** was modeled as an S_N2-type substitution of thiolate for the amide leaving group, breaking the Se−N bond

Scheme 4. Proposed Mechanistic Pathways for Ebselen Redox Scavenging under Normal and Highly Oxidizing Conditions

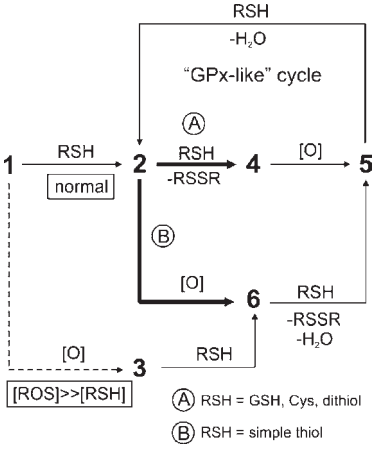

to form **6** (Figure 5 and Table 2). In **3**→$\mathbf{6_{R'}}$ the thiol proton is connected to the −NPh group by three water molecules, similar to the conversion of **14** to **15**.[45] The activation barrier for **3**→$\mathbf{6_{TS}}$ (9.2 kcal/mol) is comparable to **3**→**9**, but lower than **14**→**15** (20.5 kcal/mol)[45] because of a large solvation correction to **3**→$\mathbf{6_{TS}}$ (ΔG_{solv} = −10.3 kcal/mol). The rearranged product complex **3**→$\mathbf{6_P}$ with an Se···O interaction is slightly lower than the product complex **3**→$\mathbf{6_{P'}}$ found by following the reaction coordinate from the transition state (Table 2). The SAPE model for the subsequent step **6**→**5** (Figure 5) based on the model[45] of **15**→**17** provides an activation barrier (18.4 kcal/mol) roughly three times higher than that for **9**→**1**. In **6**→**5**, the Se···O interaction and the aromatic substituent on Se account for the higher activation barrier relative to **15**→**17** (15.8 kcal/mol).[45] Similar to the equilibrium between **15** and **16**,[45] **9** may interconvert with **6** through ring-opening via proton transfer from the −OH to the nitrogen of **9**; however, non-SAPE calculations on the isolated species **6** and **9** suggest that the equilibrium favors the seleninyl sulfide ($\Delta G_{6\rightarrow 9}$ = 4.7 kcal/mol). Additionally, thiol reduction with ring-opening (**3**→**6**) is exothermic by ∼−20 kcal/mol compared to the equilibrium predicted for **3**→**9** (Table 2) such that, despite the lower barrier for **9**→**1**, the reaction mechanism is most likely to proceed through the seleninyl sulfide **6**. Therefore, the reduction of **3** to **1** observed by Fischer et al. may be explained as the reduction of **3** to the selenenic acid **5** followed by dehydration to **1** (**1**→**3**→**6**→**5**→**1**). A similar mechanism of activity could be proposed if **3** is hydrolyzed to **10**, as suggested by Sarma and Mugesh,[38] with thiol reduction of the seleninic acid to **6** (**1**→**3**→**10**→**6**→**5**→**1**). Alternatively, some reaction conditions or stabilizing interactions with the thiol may favor shifting of the equilibrium toward **9** as found for the selenurane of SeMet oxide[86] to allow for reaction through the path **1**→**3**→**9**→**1**. Also note that given the high concentration of oxidant required to access **3** in the presence of thiols, pathways including more highly oxidized species may contribute to redox activity.

The species available to pathways under oxidative stress may also be accessible through oxidation of **2** as a potential alternate mechanism for ROS-scavenging. Step **2**→**6** was modeled using a two-water SAPE network (Figure 6 and Table 2) similar to those used for the two-electron oxidation of various organoselenium

compounds including MeSeSMe.[43] The activation barrier (21.3 kcal/mol) for **2**→**6**$_{TS}$ is consistent with the experimental second order rate constants ([O] = H_2O_2) and SAPE barriers for oxidation of ebselen and its selenol (**2**→**6** (<0.01 mM^{-1} min^{-1}); **1**→**3** (0.29 mM^{-1} min^{-1}), **4**→**5** (2.8 mM^{-1} min^{-1})[77] and significantly lower than **2**→**4** (31.7 kcal/mol). Oxidation of **2** is also energetically favorable (−34.6 vs 11.8 kcal/mol) over reduction to **4**, suggesting that ROS scavenging via the path **1**→**2**→**6**→**5**→**2** may be possible for thiols such as PhSH which do not convert **2** to the selenol **4**, albeit at much slower scavenging turnover rates than thiols such as GSH which facilitate step **2**→**4** (Scheme 4).

CONCLUSIONS

DFT-SAPE modeling of the proposed mechanistic pathways for ROS-scavenging of **1** confirms that thiol-reduction to the selenenyl sulfide **2** is favored over oxidation to the selenoxide **3** under all but extremely oxidizing conditions ([ROS] ≫ [thiol]). The selenenyl sulfide **2** is potentially a terminal product if a sufficient concentration of either ROS or thiol is not available to sustain catalysis. The high barrier for selenol regeneration (**2**→**4**) makes catalysis dependent upon the nature of the thiol reductant (Scheme 4). Dithiols and peptide-based thiols have been shown experimentally to reduce **2** to **4** thereby facilitating ROS scavenging through a GPx-like cycle (**1**→**2**→**4**→**5**→**2**). GSH and other amino acid-based thiols accelerate this reaction by increasing the electrophilicity of the sulfur center of **2** through intramolecular interactions, possibly an S···O interaction with the carbonyl of Cys or the peptide backbone; dithiols convert **2**→**4** to a unimolecular process. Simple thiols, such as thiolphenol, cannot activate the selenenyl sulfide sulfur center and, because **2**→**4** is prohibited by its high activation barrier, further reaction is proposed to follow an alternate path through the oxidation of **2** (e.g., **1**→**2**→**6**→**5**→**2**). This mechanism may explain the lack of saturation kinetics for GPx-like activity of sec-amide-based diselenides measured as a function of [thiol] because the SAPE activation barriers indicate **2**→**6** as the rate-determining step for this path. Because **2**→**6** is dependent upon the oxidant, saturation kinetics might be observed when [O] is varied. Under highly oxidizing conditions ([ROS] ≫ [thiol]), oxidation of **1** to **3** may contribute to ROS scavenging through a short-lived seleninyl sulfide **6** or, possibly, thioselenurane intermediate **9**. If the free thiol pool is depleted, **1** and its oxidized intermediates may attack protein thiols/thiolates, such as those of Zn/S transcription factors, to disrupt biochemical signal transduction. SAPE microsolvation models, which have contributed to the unraveling of the complex mechanism of **1** and other problems in solution-phase chemistry, will be expanded to these and other problems related to sulfur and selenium interactions with biochemical signaling processes in future studies.

AUTHOR INFORMATION

Corresponding Author

*E-mail: cbayse@odu.edu.

ACKNOWLEDGMENT

Funding for this project was provided by the National Science Foundation (CHE-0750413).

REFERENCES

(1) Mugesh, G.; du Mont, W.-W.; Sies, H. *Chem. Rev.* **2001**, *101*, 2125–2180.
(2) Mugesh, G.; Singh, H. B. *Chem. Soc. Rev.* **2000**, *29*, 347–357.
(3) Bhabak, K. P.; Mugesh, G. *Acc. Chem. Res.* **2010**, *43*, 1408–1419.
(4) Rayman, M. P. *Lancet* **2000**, *356*, 233–241.
(5) Tapiero, H.; Townsend, D. .; Tew, K. . *Biomed. Pharmacother.* **2003**, *57*, 134–144.
(6) Ganther, H. E. *Carcinogenesis* **1999**, *20*, 1657–1666.
(7) Ganther, H. E.; Lawrence, J. R. *Tetrahedron* **1997**, *53*, 12299–12310.
(8) Magalhães, J. P.; Church, G. M. *Exp. Gerontol.* **2006**, *41*, 1–10.
(9) Nordberg, J.; Arnér, E. S. J. *Free Radical Biol. Med.* **2001**, *31*, 1287–1312.
(10) Schewe, T. *Gen. Pharmacol.* **1995**, *26*, 1153–169.
(11) Lapchak, P. A.; Zivin, J. A. *Stroke* **2003**, *34*, 2013–2018.
(12) Ramakrishnan, N.; Kalinich, J. F.; McClain, D. E. *Biochem. Pharmacol.* **1996**, *51*, 1443–1451.
(13) Lass, A.; Witting, P.; Stocker, R.; Esterbauer, H. *BBA-Lipid Lipid Met.* **1996**, *1303*, 111–118.
(14) Masumoto, H.; Sies, H. *Chem. Res. Toxicol.* **1996**, *9*, 262–267.
(15) Daiber, A.; Zou, M.-H.; Bachschmid, M.; Ullrich, V. *Biochem. Pharmacol.* **2000**, *59*, 153–160.
(16) Sies, H.; Masumoto, H. *Adv. Pharmacol.* **1996**, *38*, 229–246.
(17) Sies, H. *Free Radical Biol. Med.* **1993**, *14*, 313–323.
(18) Jacob, C.; Maret, W.; Vallee, B. L. *Biochem. Biophys. Res. Commun.* **1998**, *248*, 569–573.
(19) Müller, A.; Cadenas, E.; Graf, P.; Sies, H. *Biochem. Pharmacol.* **1984**, *33*, 3235–3239.
(20) Müller, A.; Gabriel, H.; Sies, H.; Terlinden, R.; Fischer, H.; Römer, A. *Biochem. Pharmacol.* **1988**, *37*, 1103–1109.
(21) Ren, B.; Huang, W.; Åkesson, B.; Ladenstein, R. *J. Mol. Biol.* **1997**, *268*, 869–885.
(22) Fischer, H.; Dereu, N. *Bull. Soc. Chim. Belg.* **1987**, *96*, 757.
(23) Syed, R.; Wu, Z. P.; Hogle, J. M.; Hilvert, D. *Biochemistry* **1993**, *32*, 6157–6164.
(24) Back, T. G.; Dyck, B. P. *J. Am. Chem. Soc.* **1997**, *119*, 2079–2083.
(25) Iwaoka, M.; Tomoda, S. *J. Am. Chem. Soc.* **1994**, *116*, 2557–2561.
(26) Mugesh, G.; Panda, A.; Singh, H. B.; Punekar, N. S.; Butcher, R. J. *J. Am. Chem. Soc.* **2001**, *123*, 839–850.
(27) Bhabak, K. P.; Mugesh, G. *Chem.—Asian. J.* **2009**, *4*, 974–983.
(28) Bhabak, K. P.; Mugesh, G. *Chem.—Eur. J.* **2008**, *14*, 8640–8651.
(29) Bhabak, K. P.; Mugesh, G. *Chem.—Eur. J.* **2009**, *15*, 9846–9854.
(30) Wirth, T. *Molecules* **1998**, *3*, 164–166.
(31) Tripathi, S. K.; Patel, U.; Roy, D.; Sunoj, R. B.; Singh, H. B.; Wolmershäuser, G.; Butcher, R. J. *J. Org. Chem.* **2005**, *70*, 9237–9247.
(32) Back, T. G.; Moussa, Z. *J. Am. Chem. Soc.* **2002**, *124*, 12104–12105.
(33) Back, T. G.; Moussa, Z. *J. Am. Chem. Soc.* **2003**, *125*, 13455–13460.
(34) Singh, V. P.; Singh, H. B.; Butcher, R. J. *Chem.—Asian. J.* **2011**, *6*, 1431–1442.
(35) Back, T. G.; Kuzma, D.; Parvez, M. *J. Org. Chem.* **2005**, *70*, 9230–9236.
(36) Press, D. J.; Mercier, E. A.; Kuzma, D.; Back, T. G. *J. Org. Chem.* **2008**, *73*, 4252–4255.
(37) Sarma, B. K.; Mugesh, G. *J. Am. Chem. Soc.* **2005**, *127*, 11477–11485.
(38) Sarma, B. K.; Mugesh, G. *Chem.—Eur. J.* **2008**, *14*, 10603–10614.
(39) Pearson, J. K.; Boyd, R. J. *J. Phys. Chem. A* **2006**, *110*, 8979–8985.
(40) Pearson, J. K.; Boyd, R. J. *J. Phys. Chem. A* **2007**, *111*, 3152–3160.
(41) Pearson, J. K.; Boyd, R. J. *J. Phys. Chem. A* **2008**, *112*, 1013–1017.

(42) Musaev, D. G.; Hirao, K. *J. Phys. Chem. A* **2003**, *107*, 1563–1573.
(43) Bayse, C. A.; Antony, S. *J. Phys. Chem. A* **2009**, *113*, 5780–5785.
(44) Bayse, C. A. *J. Phys. Chem. A* **2007**, *111*, 9070–9075.
(45) Bayse, C. A. *J. Inorg. Biochem.* **2010**, *104*, 1–8.
(46) Bayse, C. A. *Org. Biomol. Chem.* **2011**, *9*, 4748–4751.
(47) Kallies, B.; Mitzner, R. *J. Mol. Model.* **1998**, *4*, 183–196.
(48) Lundin, A.; Panas, I.; Ahlberg, E. *J. Phys. Chem. A* **2007**, *111*, 9080–9086.
(49) Wu, Z.; Ban, F.; Boyd, R. J. *J. Am. Chem. Soc.* **2003**, *125*, 6994–7000.
(50) Yeung, C. S.; Ng, P. L.; Guan, X.; Phillips, D. L. *J. Phys. Chem. A* **2010**, *114*, 4123–4130.
(51) Arroyo, S. T.; Garcia, A. H.; Martin, J. A. S. *J. Phys. Chem. A* **2009**, *113*, 1858–1863.
(52) Long, B.; Zhang, W.-J.; Tan, X.-F.; Long, Z.-W.; Wang, Y.-B.; Ren, D.-S. *J. Phys. Chem. A* **2011**, *115*, 1350–1357.
(53) Taxak, N.; Parmar, V.; Patel, D. S.; Kotasthane, A.; Bharatam, P. V. *J. Phys. Chem. A* **2011**, *115*, 891–898.
(54) Wang, B.; Cao, Z. *J. Phys. Chem. A* **2010**, *114*, 12918–12927.
(55) Prabhakar, R.; Vreven, T.; Morokuma, K.; Musaev, D. G. *Biochemistry* **2005**, *44*, 11864–11871.
(56) Frisch, M. J.; Trucks, G. W.; Schlegel, H. B.; Scuseria, G. E.; Rob, M. A.; Cheeseman, J. R.; Montgomery, J. A.; Vreven, T.; Kudin, K. N.; Burant, J. C.; Millam, J. M.; Iyengar, S. S.; Tomasi, J.; Barone, V.; Mennucci, B.; Cossi, M.; Scalmani, G.; Rega, N.; Petersson, G. A.; Nakatsuji, H.; Hada, M.; Ehara, M.; Toyota, K.; Fukuda, R.; Hasegawa, J.; Ishida, M.; Nakajima, T.; Honda, Y.; Kitao, O.; Nakai, H.; Klene, M.; Li, X.; Knox, J. E.; Hratchian, H. P.; Cross, J. B.; Bakken, V.; Adamo, C.; Jaramillo, J.; Gomperts, R.; Stratmann, R. E.; Yazyev, O.; Austin, A. J.; Cammi, R.; Pomelli, C.; Ochterski, J. W.; Ayala, P. Y.; Morokuma, K.; Voth, G. A.; Salvador, P.; Dannenberg, J. J.; Zakrzewski, V. G.; Dapprich, S.; Daniels, A. D.; Strain, M. C.; Farkas, O.; Malick, D. K.; Rabuck, A. D.; Raghavachari, K.; Foresman, J. B.; Ortiz, J. V.; Cui, Q.; Baboul, A. G.; Clifford, S.; Cioslowski, J.; Stefanov, B. B.; Liu, G.; Liashenko, A.; Piskorz, P.; Komaromi, I.; Martin, R. L.; Fox, D. J.; Keith, T.; Al-Laham, M. A.; Peng, C. Y.; Nanyakkara, A.; Challacombe, M.; Gill, P. M. W.; Johnson, B.; Chen, W.; Wong, M. W.; Gonzalez, C.; Pople, J. A. *Gaussian 03*, Revision D.01; Gaussian, Inc.: Wallingford, CT, 2004.
(57) Adamo, C.; Barone, V. *J. Chem. Phys.* **1998**, *108*, 664–675.
(58) Bayse, C. A.; Antony, S. *Main Group Chem.* **2007**, *6*, 185–200.
(59) Kona, J.; Fabian, W. M. F. *J. Chem. Theory Comput.* **2011**, *7*, 2610–2616.
(60) Hurley, M. M.; Pacios, L. F.; Christiansen, P. A.; Ross, R. B.; Ermler, W. C. *J. Chem. Phys.* **1986**, *84*, 6840–6853.
(61) Wadt, W. R.; Hay, P. J. *J. Chem. Phys.* **1985**, *82*, 284–298.
(62) Dunning, T. H. *J. Chem. Phys.* **1971**, *55*, 716–723.
(63) Dunning, T. H. *J. Chem. Phys.* **1970**, *53*, 2823–2833.
(64) Tomasi, J.; Mennucci, B.; Cammi, R. *Chem. Rev.* **2005**, *105*, 2999–3094.
(65) Cioslowski, J. *J. Am. Chem. Soc.* **1989**, *111*, 8333–8336.
(66) Haenen, G. R.; De Rooij, B. M.; Vermeulen, N. P.; Bast, A. *Mol. Pharmacol.* **1990**, *37*, 412–422.
(67) Maiorino, M.; Roveri, A.; Coassin, M.; Ursini, F. *Biochem. Pharmacol.* **1988**, *37*, 2267–2271.
(68) Zhao, R.; Holmgren, A. *J. Biol. Chem.* **2002**, *277*, 39456–39462.
(69) Wagner, G.; Schuch, G.; Akerboom, T. P. M.; Sies, H. *Biochem. Pharmacol.* **1994**, *48*, 1137–1144.
(70) Rooseboom, M.; Commandeur, J. N. M.; Floor, G. C.; Rettie, A. E.; Vermeulen, N. P. E. *Chem. Res. Toxicol.* **2001**, *14*, 127–134.
(71) Cotgreave, I. A.; Morgenstern, R.; Engman, L.; Ahokas, J. *Chem.-Biol. Interact.* **1992**, *84*, 69–76.
(72) Glass, R. S.; Farooqui, F.; Sabahi, M.; Ehler, K. W. *J. Org. Chem.* **1989**, *54*, 1092–1097.
(73) Bayse, C. A.; Baker, R. A.; Ortwine, K. N. *Inorg. Chim. Acta* **2005**, *358*, 3849–3854.
(74) Reed, A. E.; Curtiss, L. A.; Weinhold, F. *Chem. Rev.* **1988**, *88*, 899–926.
(75) Minyaev, R. M.; Minkin, V. I. *Can. J. Chem.* **1998**, *76*, 776–788.
(76) Bayse, C. A.; Pavlou, A. *Org. Biomol. Chem.* DOI: 10.1039/C1OB05827D.
(77) Morgenstern, R.; Cotgreave, I. A.; Engman, L. *Chem.-Biol. Interact.* **1992**, *84*, 77–84.
(78) Goto, K.; Nagahama, M.; Mizushima, T.; Shimada, K.; Kawashima, T.; Okazaki, R. *Org. Lett.* **2001**, *3*, 3569–3572.
(79) Cowan, E. A.; Oldham, C. D.; May, S. W. *Arch. Biochem. Biophys.* **2011**, *506*, 201–207.
(80) Arai, K.; Dedachi, K.; Iwaoka, M. *Chem.—Eur. J.* **2011**, *17*, 481–485.
(81) Wolinski, K.; Hinton, J. F.; Pulay, P. *J. Am. Chem. Soc.* **1990**, *112*, 8251–8260.
(82) Bayse, C. A. *Inorg. Chem.* **2004**, *43*, 1208–1210.
(83) Bayse, C. A. *J. Chem. Theory Comput.* **2005**, *1*, 1119–1127.
(84) Allenmark, S. *Chirality* **2008**, *20*, 544–551.
(85) Sato, S.; Matsuo, M.; Nakahodo, T.; Furukawa, N.; Nabeshima, T. *Tetrahedron Lett.* **2005**, *46*, 8091–8093.
(86) Ritchey, J. A.; Davis, B. M.; Pleban, P. A.; Bayse, C. A. *Org. Biomol. Chem.* **2005**, *3*, 4337–4342.